Hindawi Publishing Corporation
Journal of Energy
Volume 2013, Article ID 394512, 9 pages
http://dx.doi.org/10.1155/2013/394512

Research Article

A Low-Cost Polytetrafluoroethylene-Framed TiO_2 Electrode Decorated with Oleic Acid-Capped CdSe Quantum Dots for Solar Cell

Delele Worku Ayele,[1] Wein-Nien Su,[2] and Bing-Joe Hwang[1,3]

[1] *Department of Chemical Engineering, National Taiwan University of Science and Technology, Taipei 106, Taiwan*
[2] *Graduate Institute of Engineering, National Taiwan University of Science and Technology, Taipei 106, Taiwan*
[3] *National Synchrotron Radiation Research Center, Hsinchu 300, Taiwan*

Correspondence should be addressed to Wein-Nien Su; wsu@mail.ntust.edu.tw and Bing-Joe Hwang; bjh@mail.ntust.edu.tw

Received 13 February 2013; Revised 30 May 2013; Accepted 3 June 2013

Academic Editor: Ching Yuan Chang

Colloidal CdSe QDs have been assembled, as quantum dot-sensitized solar cells (QDSSCs), on a novel architecture comprising a polytetrafluoroethylene- (PTFE-) framed TiO_2 electrode for the first time. CdSe QDs are anchored on the surface of the film using a linker molecule (3-mercaptopropionic acid, MPA). The resulting photoelectrode comprises a TiO_2 compact layer and a PTFE-framed structural layer with average respective thicknesses of 2 μm for the compact layer and either 23 μm or 28 μm for the PTFE-framed structural layer. UV-vis absorption spectra show that more CdSe quantum dots are anchored on the surface of the modified with MPA TiO_2 film compared to direct absorption onto an unmodified film. Energy conversion efficiencies of up to 0.18% can be achieved with cells prepared from a TiO_2 (25 μm)/MPA/CdSe QD electrode. Electrochemical impedance measurements show that the recombination resistance is relatively higher for a cell assembled with TiO_2 (25 μm)/MPA/CdSe QD photoanode than with TiO_2 (25 μm)/CdSe QD resulting in an increase of cell efficiency. The PTFE-framed structure along with the compact layer is a new approach to QDSSC application that provides a tunable film thickness and a cost-effective preparation technique for the large-scale production of the photoanode.

1. Introduction

Dye-sensitized solar cells (DSSCs) have attracted much attention as a promising alternative energy source to conventional solid-state junction solar cells due to their low cost, low impact on the environment, and high efficiency [1]. In DSSCs, the dye adsorbed on the surface of mesoporous TiO_2 films [2] is responsible for the light absorption and subsequent electron transfer reactions and is thus regarded as one of the key factors determining the conversion efficiency from light to electricity [3, 4]. Over 11% efficiency has been reported with the use of ruthenium-based sensitizer complexes [1]. In recent years, in addition to the organic sensitizers commonly used for DSSCs, inorganic semiconductors which absorb visible light have also been used as light-harvesting materials for solar cells [3–5]. Inorganic semiconductor quantum dots (QDs), such as CdS and CdSe, have been employed as sensitizers, mainly due to their specific advantages over conventional dyes [6–9]; for instance, the size quantization effect allows tuning of the band energy and visible response by simply varying the QD size [10, 11]. Another advantage is that these QDs open new ways to utilize hot electrons or generate multiple charge carriers with one single photon through the impact ionization effect [12, 13]. Thus, it is possible to obtain a much higher conversion efficiency by utilizing the multiple excitons generation possibilities offered by QDs [14]. Despite the advantage known for a QD sensitizer, up-to-date studies on quantum dot-sensitized solar cells (QDSSCs) are relatively few compared with conventional Ru-based DSSCs, and their efficiencies are also so far unsatisfactory. Recently, QDSSCs with power conversation efficiency more than 4% have been reported [15–17]. The energy conversion efficiencies reported

for an oleic acid-capped QD-sensitized DSSCs are still low (less than 1%) [18]. The problems encountered in fabricating a QDSSC include the assembly of the QDs into a mesoporous TiO_2 matrix [3, 19] and the selection of an efficient electrolyte in which the QDs can run stably without serious degradation [20]. Compared to iodide/triiodide (I^-/I^{3-}) electrolyte, using polysulfide electrolyte and CdS as a sensitizer shows better stability with a much higher short circuit current and IPCE (~80%) value [20]. Two methods are commonly employed to assemble QDs into a mesoporous thin film. The first is to assemble preprepared QDs using bifunctional linkers [3], and the other is by *in situ* deposition from precursor solutions using successive chemical bath deposition [8].

Chemical bath deposition [8, 21, 22] involving nucleation and growth leads to a high coverage of QDs on the TiO_2 surface but has the disadvantage of not giving good control of the size distribution of the deposited QDs. On the other hand, the attachment of colloidal QDs using a molecular linker leads to precise morphological characteristics (i.e., shape and size) of the semiconductor nanocrystals—leading to enhanced properties when compared to CBD [3, 23–25].

Similar to DSSC, under the illumination of solar light; QDs are excited and electrons are produced. To generate meaningful electrical power from QDSSC, the electrons need to pass four important interfaces of QDSSCs that are TiO_2/FTO, QDs/TiO_2, QDs/electrolyte, and the electrolyte/counter electrode. The nanoporous nature of the TiO_2 layer provides a high surface area that is of great importance to the efficient photon-to-electricity conversion because it first enhances QD loading and then solar light absorption [26]. However, it also provides abundant TiO_2 surface sites (direct route) and bare FTO conducting sites (indirect route), where the photoinjected electrons may recombine with species of electrolyte [27]. Such recombination will cause the loss of the photocurrent so that the photovoltaic performance of the device is seriously decreased [28].

In previous reports, it was suggested that putting an additional compact layer of TiO_2 between the fluorine-doped tin oxide (FTO) glass and the mesoporous TiO_2 layer to prevent the recombination of the photogenerated charges at the boundary seen in DSSC would also increase the contact between FTO and TiO_2 films [27–29]. Therefore, we applied a hybrid film comprising a structural layer (a mixture of polytetrafluoroethylene (PTFE) and TiO_2) on the compact layer of TiO_2 on the FTO glass.

The PTFE-framed structure helped to increase dye absorption to achieve an energy conversion efficiency of 9.04% for the dye-sensitized solar cell [30, 31]. Moreover, the use of PTFE in the structural layer allows the cost-effective preparation of large surface area TiO_2 electrodes with a tunable thickness [30, 31]. To the best of our knowledge, a photoanode with such an architecture represents a new approach for QDSSC applications.

We prepared different QDSSC using two strategies to attach the colloidal CdSe QDs onto the PTFE-framed TiO_2 surface—with a linker molecule (3-mercaptopropionic acid (MPA)) and by direct adsorption without linker. We further discussed the electrochemical properties of the cells prepared by the two methods of anchoring the CdSe QDs onto the TiO_2 surface and the resulting effects on the performance of QDSSCs. In this report, polysulfide electrolyte was used as the redox couple to regenerate the photoexcited holes in the QDs with Pt being used as a counter electrode.

2. Experimental

2.1. Chemicals. Selenium powder (99.70%), sodium sulfite (>95%), and n-hexane (>99%) were all from Acros. Sulfur (99.99%), potassium chloride (99%), sodium sulfide (90%), anhydrous acetonitrile (99.9%), 3-mercaptopropionic acid (MPA, 99%), N-dimethylformamide (>99%), titanium butoxide (97%), isopropanol (99.7%), ethanol (>99%), and oleic acid (65–88%) were all from Aldrich. Cadmium acetate dihydrate (>99%) was from J. T. Baker, and sodium hydroxide (>95%) was from Shimakyus Pure Chemicals. All chemicals were used as received without further purification. Fluorine-doped tin oxide (FTO) glass (≤14 Ω/square) was from Pilkington. Polytetrafluoroethylene (PTFE, DuPont) and TiO_2 P25 (Degussa) were also used.

2.2. Synthesis of CdSe QDs. CdSe QDs were prepared using a microwave-based protocol developed by our group [32]. In a typical synthesis, NaOH (0.72 g) and oleic acid (8 mL) were dissolved in aqueous solvents. $Cd(Ac)_2{\cdot}2H_2O$ (0.27 g) was separately dissolved in 10 mL deionized water and added to this solution under stirring, followed by addition of Na_2SeSO_3 (10 mL) solution. The resulting solution was heated in a microwave system at 100 W and 80°C, for 5 mins to grow the CdSe QDs. The oleic acid-capped CdSe QDs were washed and collected via centrifugation and decantation of the supernatant.

2.3. Preparation of TiO_2 Nanoparticles. TiO_2 nanoparticles were fabricated by a typical hydrothermal method [30, 33]. A 9.25 mL sample of tetrabutyl titanate ($Ti(OC_4H_9)_4$) was mixed with 2-propanol (2.5 mL), and the mixture was slowly added to a solution comprising deionized water (62 mL) and acetic acid (20 mL) in an ice bath with stirring. The solution was then heated to 80°C and stirred vigorously for 8 h. TiO_2 nanoparticles, to be used as a TiO_2 paste, were grown under hydrothermal conditions in an autoclave for 12 h with the autoclave temperatures set at 190°C.

2.4. Fabrication of CdSe QDSSCs. For the preparation of photoelectrodes, we used the technique developed by our group for the preparation of FTO/compact TiO_2 layer/PTFE-farmed TiO_2 films [18, 34]. To fabricate the PTFE-framed TiO_2 films, the glass plate was coated with the TiO_2 paste using a glass rod, dried in oven at 80°C for 15 min and then sintered at 500°C for 30 min to form a compact layer. On top of the compact layer, a second structural layer was built by coating a paste of PTFE and TiO_2 P25 mixed with some ethanol. The coated plate was dried in oven at 80°C for 15 min and then sintered at 500°C for 60 min to form the PTFE-framed TiO_2 film. A photoanode (i.e., a TiO_2 film comprising the compact and structural layers) with different average

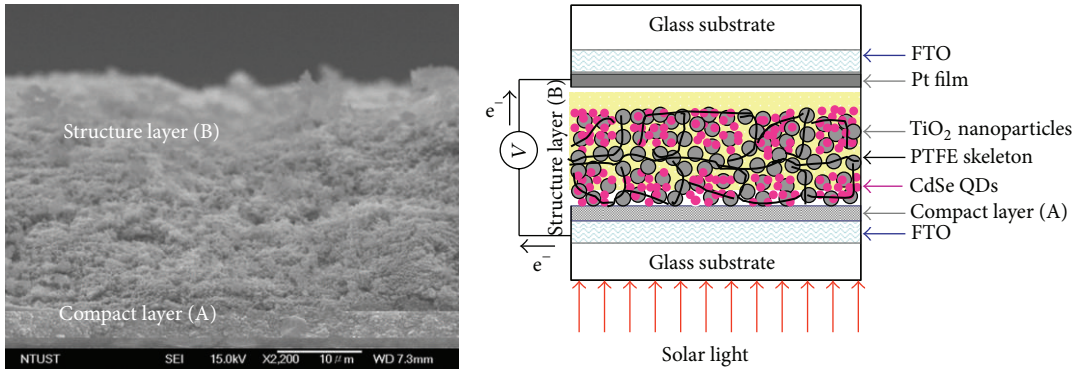

(a) (b)

FIGURE 1: (a) SEM cross-section of compact layer (A) and structure layer (B) of the film. Scale bare 10 μm. (b) A schematic representation of QDSSC device (FTO/compact TiO_2 layer/PTFE-framed TiO_2 film/CdSe QDs).

thicknesses of the structural layer (23 μm and 28 μm) and the same average thickness of compact layer (2 μm) giving total thicknesses of 25 and 30 μm was prepared. Two modes of attachment for CdSe QD on the films were employed. The first used linker molecules to attach CdSe QDs to the surface. The film's surface was modified by immersion in a 0.5 M MPA acetonitrile solution for 12 hrs prior to rinsing with acetonitrile followed by further immersion in 0.26 mM CdSe QD toluene solution for 48 hrs and a final rinse in toluene: this electrode was designated as TiO_2/MPA/CdSe QD. The second electrode was prepared without linker molecules. The unmodified TiO_2 film was directly immersed in a CdSe QD (0.26 mM) toluene solution for 48 hrs and then rinsed in toluene: this electrode was designated as TiO_2/CdSe QD. Polysulfide electrolyte solutions were prepared following the literature procedure [20]. The typical composition of the polysulfide electrolyte was Na_2S (0.5 M), S (2 M), and KCl (0.2 M) in the mixture of solvents (3 mL of deionized water and 7 mL of methanol). Finally, a sandwich-type cell was fabricated by clamping the polysulfide electrolyte between the QD-sensitized photoanode and the Pt counter electrode (a platinum sputtered FTO plate) with two clips. The active area of all cells was 0.5 cm^2.

2.5. Characterization. UV-visible absorption spectra were obtained using Jasco-560 UV/vis Spectrophotometer. The cross-section of the electrode was measured using scanning electron microscopy (FE-SEM, JEOL JSM-6500F, Tokyo, Japan). The photocurrent-voltage (I-V) curves were measured under an illumination from a solar simulator at one sun (AM 1.5, 100 mW cm^{-2}). An Oriel 500 W xenon arc lamp and Keithley 2400 electrometer were used during the measurements of IPCE. Electrochemical impedance spectra (EIS) were measured with an Autolab, PGSTAT302N Potentiostat/Galvanostat (frequency range: 10 micro-Hz to 1 MHz, maximum output voltage: 30 V, and current range: 10 nA to 1 A) under illumination (AM 1.5 100 mW cm^{-2}) by applying different potentials. Electrochemical impedance spectra were fitted with use of Z-View software (Solartron Analytical). X-ray diffraction (XRD) measurements (D2 Phaser, Bruker, Germany) were recorded using a Cu Kα radiation source.

3. Results and Discussion

In Figure 1(a), the SEM cross-section shows that the compact (A) and structural layers (B) have average thicknesses of 2 μm and 23 μm, respectively. Figure 1(b) shows a schematic representation of the QDSSC device, depicting the FTO, the compact TiO_2 layer, the PTFE skeleton in PTFE-framed TiO_2 structure layer, the absorbed CdSe QDs on a TiO_2 film, and the counter electrode. Basically, the compact layer was constructed to create more contact between FTO and the PTFE-framed TiO_2 structure and also to avoid recombination and short circuiting at the FTO. The PTFE-framed TiO_2 structural layer (B) provides a large surface area [31] on which the CdSe quantum dots are absorbed and where light harvesting and charge separation take place. The separated electrons and holes are, respectively, conducted through TiO_2 to the FTO and through polysulfide electrolytes to the Pt cathode.

The sintering effect on the PTFE-framed TiO_2 structural layer was also analyzed by comparing with the original TiO_2 paste. The X-ray diffraction patterns of the TiO_2 paste used for compact layer (A) formation and the structural layer (B) are shown in Figure 2. Anatase and rutile phase peaks are marked as "A" and "R," respectively. Both samples consist of anatase and rutile phase. However, the rutile phase of TiO_2 films is more pronounced in the structure layer (B) than in the TiO_2 paste as a result of sintering. In general, the XRD patterns of both samples are almost identical.

In the past years, PTFE-framed TiO_2 structure for DSSC has been developed in our group [30, 31]. The study shows that the pure PTFE powder exhibits particle size in the range of 30–100 nm before sintering, and the morphology becomes column-like after sintering at 500°C for 60 minutes. PTFE formed as a highly porous skeleton which enables to hold more TiO_2 particles, a requirement for the decoration of QDs. The optimal mixing proportion of TiO_2 and PTFE was determined as 50/50 wt.% [31]. The PTFE skeleton is also

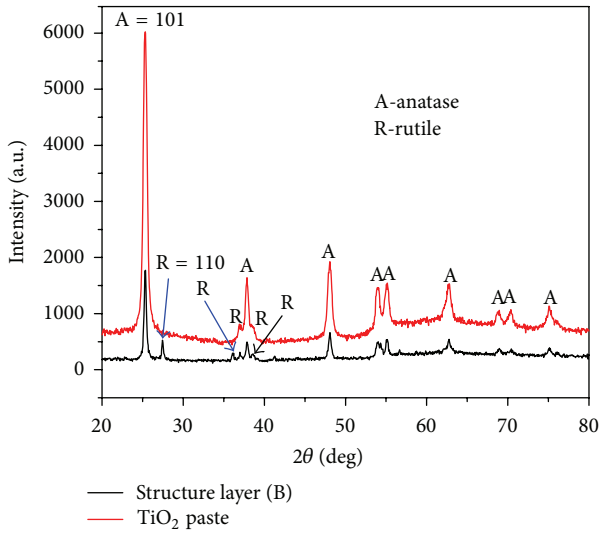

Figure 2: The XRD spectra of TiO_2 paste used for the preparation of compact layer and sintered structure layer.

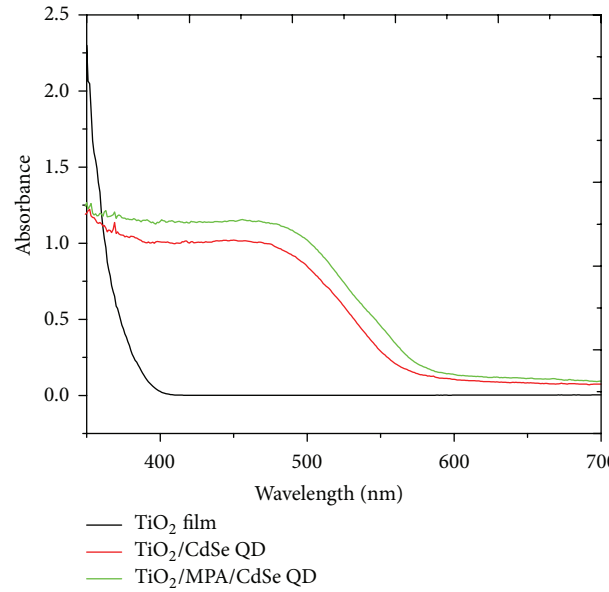

Figure 3: UV-visible absorption spectra of pristine TiO_2 film, TiO_2/CdSe QD electrode, and TiO_2/MPA/CdSe QD electrode. The total TiO_2 film thickness is 25 μm.

supposed to contribute the necking of TiO_2 in the PTFE-framed TiO_2 electrode. In this report, the structure of PTFE remained mainly intact for sintering temperatures up to 500°C [31].

The assembly of presynthesized colloidal QD is a popular method used to fabricate QD-sensitized electrodes. For maximum CdSe QD loading, the TiO_2 film was first modified with mercaptopropionic acid MPA linker, and then it was immersed in CdSe QD solution. The mechanism is based on well-known hard and soft acids and bases theories [35], and the ligands exchange between OA and MPA linker takes place. The hard-hard or soft-soft molecules or ions form a strong binding, owing to the polarizability of electron cloud. The Cd^{2+} and Se^{2-} ions are classified as soft ions and have stronger interaction with soft "–SH (from MPA)" but not hard "–COOH (from OA or MPA) [35]." Therefore, during the period of dynamic dissociation and association of ligand, the MPA molecule can form rather strong bonding with CdSe (soft –SH from MPA and soft Cd^{2+} or Se^{2-} ions) than –COOH. The different strengths of bonding enhance the ligand exchange between OA and MPA. After OA and MPA ligand exchange, MPA links QD and TiO_2 by a thiol (–SH) and carboxylate group (–COOH), respectively. Hence, the modification of CdSe QDs capping plays a key role to improve CdSe QDs loading on the TiO_2 films and then the performance of QDSSC.

Thus, for comparison, colloidal CdSe QDs were deposited on 3-mercaptopropionic acid- (MPA-) modified and pristine TiO_2 films separately, denoted as TiO_2/MPA/CdSe QD and TiO_2/CdSe QD, respectively. The absorption of CdSe QD on a TiO_2 film was evaluated using UV-vis absorbance spectroscopy. Figure 3 shows representative UV-vis absorbance spectra of CdSe-sensitized TiO_2 electrodes, prepared with and without MPA modification. It is found that the absorbance of the TiO_2/MPA/CdSe QD electrode was higher in comparison with that of TiO_2/CdSe QD under the same deposition conditions, indicating that a bifunctional molecular linker such as 3-mercaptopropionic acid (MPA, $HOOC–CH_2–CH_2–SH$) can improve the coverage of TiO_2 surface with quantum dots [3, 19, 36]. 3-mercaptopropionic acids (MPA) have both carboxylate and thiol functional groups at the opposite terminals of the structure, which can facilitate the binding between CdSe quantum dots and TiO_2 surfaces [3, 19, 36]. The presence of thiol terminal groups helps incorporating and stabilizing CdSe QDs, decreasing the desorption events of CdSe QDs during rinsing, and thereby increasing the deposition amount of CdSe QDs [3, 19, 36]. Use of such linker molecules ensures monolayer coverage of the CdSe QDs film within the TiO_2 network. For the direct deposition of OA-capped CdSe QDs on the surface of PTFE-framed TiO_2 nanoparticles, since the hydrophilic (–COOH) part of OA binds colloidal CdSe QDs with the hydrophobic part of oleic acid (OA) towards the surface of TiO_2 nanoparticles, it results in a weak binding between CdSe QDs and TiO_2 surface. As a result, most of the CdSe QDs were removed during rinsing, leading to a lower UV-visible absorption compared with MPA-modified TiO_2 surface (in Figure 3). Therefore, it is reasonable to suggest that surface modification of TiO_2 films by MPA enhances the coverage of TiO_2 with quantum dots that have shown an increase in UV-visible absorption of CdSe QDs (Figure 3). The incorporated amount of CdSe QDs in the TiO_2 film can be evaluated by the absorbance at the first absorption peak using Beer-Lambert's law [18].

Photocurrent-voltage (I-V) curves for QDSSCs were measured under the illumination of one sun (AM 1.5, 100 mW cm^{-2}) as presented in Figure 4(a). These cells were made with different total thicknesses (as indicated in Figure 4(a)) of the TiO_2 film (compact and structure layers)

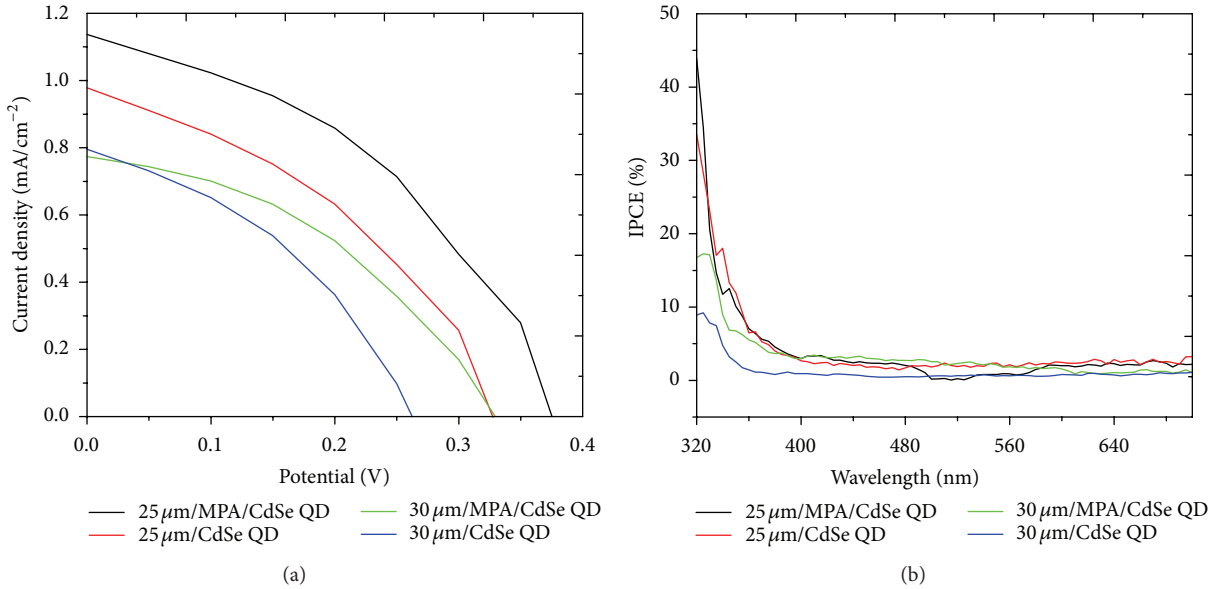

Figure 4: I-V characteristics (a) and the IPCE spectra (b) of the TiO_2 (25 and 30 μm)/MPA/CdSe QD and TiO_2 (25 and 30 μm)/CdSe QD cells in polysulfide electrolyte.

Table 1: Parameters obtained from photocurrent-voltage (I-V) measurement of the TiO_2/CdSe QD and TiO_2/MPA/CdSe QD QDSSC cells with different TiO_2 film thicknesses indicated in brackets.

Electrode	I_{max} (mA)	V_{max} (mV)	I_{sc} (mA)	P_{max} (mW)	J_{sc} (mA/cm^2)	V_{oc} (mV)	FF (%)	η (%)
TiO_2 (25 μm)/MPA/CdSe QD	0.36	249.94	0.57	0.09	1.14	399.93	39.25	0.18
TiO_2 (25 μm)/CdSe QD	0.32	199.94	0.49	0.06	0.98	349.91	36.90	0.13
TiO_2 (30 μm)/MPA/CdSe QD	0.26	199.93	0.38	0.05	0.77	349.93	38.67	0.11
TiO_2 (30 μm)/CdSe QD	0.27	149.91	0.39	0.04	0.80	249.96	40.60	0.08

and with different methods of attaching CdSe QDs to their surfaces. The thickness of the compact layer (2 μm) was constant for all photoanodes, while the thickness of the structural layer was either 23 or 28 μm. The solar energy-to-electricity conversion efficiency (η) of QDSSC was calculated by the following equation:

$$\eta = \frac{\mathrm{FF} J_{sc} V_{oc}}{P_{in}} \times 100\%, \quad (1)$$

where J_{sc} is the short-circuit photocurrent density, V_{oc} is the open circuit voltage, P_{in} is the light power per unit area, and FF is the fill factor which is calculated by the following equation:

$$\mathrm{FF} = \frac{P_{max}}{J_{sc} V_{oc}} = \frac{I_{max} V_{max}}{J_{sc} V_{oc}}, \quad (2)$$

where I_{max} and V_{max} are the current and potential at the maximum power point, respectively, in I-V curves of the solar cells. The I-V characterization was conducted under P_{in} of 100 mW cm^{-2} for the η calculation. The open circuit potential (V_{oc}), short circuit current density (J_{sc}), fill factor (FF), and the total energy conversion efficiency (η) of these cells are summarized in Table 1. For the cell in which the electrode was prepared by direct absorption, TiO_2 (25 μm)/CdSe QD cell, the efficiency (η) was 0.13%, but a higher value, η = 0.18%, was obtained for the cell in which its electrode is made via the MPA modification, TiO_2 (25 μm)/MPA/CdSe QD cell. This result is attributed to the higher incorporation and better coverage of CdSe QDs on MPA-modified TiO_2 surface as seen in UV-vis absorption spectra, which leads to higher values of I_{sc}, V_{oc}, and FF of the MPA-modified cell as compared with the corresponding unmodified cell. For example, the FFs measured for the TiO_2 (25 μm)/MPA/CdSe cells are 39.25% higher than those of the TiO_2 (25 μm)/CdSe cells (FF = 36.90%) and are responsible for the higher efficiency of the MPA-modified cells. It is inferred that the presence of the MPA layer helped to achieve a better coverage of CdSe QD on the MPA-TiO_2 surface and reduced the direct contact of TiO_2 to the electrolyte, preventing recombination of excited electrons from the conduction band of TiO_2 with the electrolyte, and thereby leading to the higher FF. Furthermore, a better light to electricity conversion efficiency was obtained for a solar cell assembled with TiO_2 film thicknesses of 25 μm than with 30 μm. This is may be due to the difficulty of electron transfer from CdSe QDs to FTO as a result of the higher thickness of the films. The electron collection efficiency and the electron recombination ratio can be determined from the IPCE value [29]. The IPCE is defined as the ratio of the number of electrons in the external circuit

produced by an incident photon at a given wavelength. The IPCE was measured as a function of wavelength. The number of incident photons on the device was calculated for each wavelength by using a calibrated Si-diode as a reference. The incident photon-to-current conversion efficiency (IPCE) of QDSSC, a measure of the external quantum efficiency, is defined as [19, 29]

$$\begin{aligned} \text{IPCE} &= \frac{\text{number of collected electrons}}{\text{number of incident photons}} = \frac{hcJ_{sc}}{e\lambda P_{in}}, \\ \text{IPCE}\,(\%) &= \frac{1240 \times J_{sc}\left(\text{A/cm}^2\right)}{\lambda\ (\text{nm}) \times P_{in}\ \left(\text{W/cm}^2\right)} \times 100, \end{aligned} \tag{3}$$

where λ, e, h, and c are the incident wavelength, elementary charge, Planck constant, and speed of light, respectively [29]. Using (3), the IPCE values of the QDSSCs with four different photoanodes as a function of the illumination wavelength are shown in Figure 4(b). The QDSSC with the TiO_2 (25 μm)/MPA/CdSe electrode showed the highest IPCE value among all other electrodes. The reasons for this difference are varied and may be linked to the factors that determine IPCE, namely, the light-harvesting efficiency (LHE) of the CdSe quantum dots, the charge injection yield or efficiency (φ_{inj}) from the excited CdSe quantum dots to the TiO_2 conduction band, and the charge collection efficiency (η_{coll}) of the system. Therefore, the IPCE in terms of these parameters can be rationalized using the following equation [29, 37]:

$$\text{IPCE}\,(\%) = \text{LHE}\,(\%)\,\varphi_{inj}\,\eta_{coll}. \tag{4}$$

Based on (4), three major parameters such as light harvesting, charge injection, and charge collection determine the IPCE value of QDSSC [38]. The parameters LHE and φ_{inj} are directly related to the CdSe QDs loading on the TiO_2 surface of the photoanode. As aforementioned, a photoanode with MPA-modified TiO_2 films showed a higher CdSe QDs absorption (Figure 3). Although the bifunctional linker (MPA) helps the coverage of TiO_2 surface by CdSe quantum dots, the longer molecular chain in MPA leads to the decrease of electron injection [25, 39, 40]. This effect has been shown clearly in the value of J_{sc} for the cell with TiO_2 (30 μm)/CdSe electrode, in which a cell with TiO_2 (30 μm)/CdSe electrode has higher J_{sc} than TiO_2 (30 μm)/MPA/CdSe electrode (Figure 4(a) and Table 1). Moreover, charge injection from excited state (CdSe QDs*) into the conduction band of TiO_2 occurs in competition with the radiative and nonradiative modes of deactivation of the excited state [37]. Another dominating factor that influences the IPCE value of QDSSC could be the electron collection efficiency (η_{coll}) [41]. In our case, the electron collection efficiency may be affected by the thickness of the TiO_2 films. As shown in I-V curve (Figure 4(a)) and IPCE (Figure 4(b)), QDSSC with TiO_2 (30 μm)/CdSe electrode resulted in a lower IPCE value and conversation efficiency than TiO_2 (25 μm)/MPA/CdSe electrodes. Insights of this issue and preparation of TiO_2 films with lower thickness are underway, and their results will be reported in the future. In general, the electron collection efficiency and the electron recombination ratio will determine the IPCE of the QDSSC.

In order to reveal the interfacial reactions of photoexcited electrons in our QDSSCs, electrochemical impedance spectroscopy (EIS) analysis of the as-prepared QDSSC with a total film (compact and structure layer) thickness 25 μm was measured. Figure 5 shows the typical Nyquist plots obtained at different applied voltages (0.3, 0.4, and 0.5 V) under light illumination of one sun (AM 1.5, 100 mW cm^{-2}) for TiO_2 (25 μm)/MPA/CdSe QD (a) and TiO_2(25 μm)/CdSe QD (b) cells.

Two semicircles exist in the high-frequency (10^3–10^6 Hz) region and the middle-frequency (1–10^3 Hz) region for both cells. In the high-frequency region or the first semicircle where the phase is zero, the ohmic series resistance (R_s) of the FTO layer, the Pt layer, and the electrolyte can be determined [3, 4, 30]. The middle-frequency region or the second semicircle is correlated with heterogeneous electron transfer at TiO_2/QD/electrolyte interface, which consists of the chemical capacitance and recombination resistance [31, 34].

The charge transfer resistance for the nanoparticle (TiO_2) cell has exponential dependence on bias [36]. As seen in Figure 5, the transport and charge transfer processes in the PTFE-framed TiO_2 films, prominent at low bias, show up as a straight line followed by the big arc at intermediate frequencies, respectively. Moreover, the size of a high frequency arc depends strongly on the applied bias potential [42], while an intermediate frequency range is visible at medium to higher forward bias [36, 38, 42]. As seen in Figure 5, as bias is applied, the high-frequency semicircle remains unchanged, while the lower-frequency semicircle shrinks. The values of series resistance (R_s) and recombination resistance (R_r) were evaluated by fitting the spectra, using the equivalent circuit shown in the inset of Figure 5(a) for both cells, in which the measurements were carried out at various applied voltages. The equivalent circuit used for fitting the EIS for both cells is shown in the inset Figure 5(a): R_s is the series resistance, R_1 is the recombination resistance (R_r), CPE1 is a constant phase element representing the chemical capacitance ($C\mu$), R_2 stands for the charge transfer resistance between the counter electrode and the redox couple, and CPE2 takes into account the capacitance of the electrolyte counter electrode interface [34, 43, 44].

The results in Figure 5 clearly show that the value of recombination resistance decreases with an increase in applied voltage for both cells. For further comparison and analysis between the two electrodes, the EIS spectra measured at 0.4 V applied voltage, which is nearly equal to the open circuit voltage, were taken for both cells. With both cells (TiO_2/MPA/CdSe QD and TiO_2/CdSe QD) at 0.4 V applied voltage, the values of R_s, R_1, and R_2 were found to be 89 Ω, 292 Ω, and 41.61 Ω, respectively, for the TiO_2/MPA/CdSe QD cell and 64.57 Ω, 99.2 Ω, and 34.41 Ω, respectively, for the TiO_2/CdSe QD cell. The R_s value of both cells is nearly the same. However, the value of recombination resistance at the electrode/electrolyte for TiO_2/MPA/CdSe QD cell is relatively higher than that of TiO_2/CdSe QD cell, indicating that the charge recombination in TiO_2/MPA/CdSe QD cell is suppressed as compared to TiO_2/CdSe QD cell. This implies

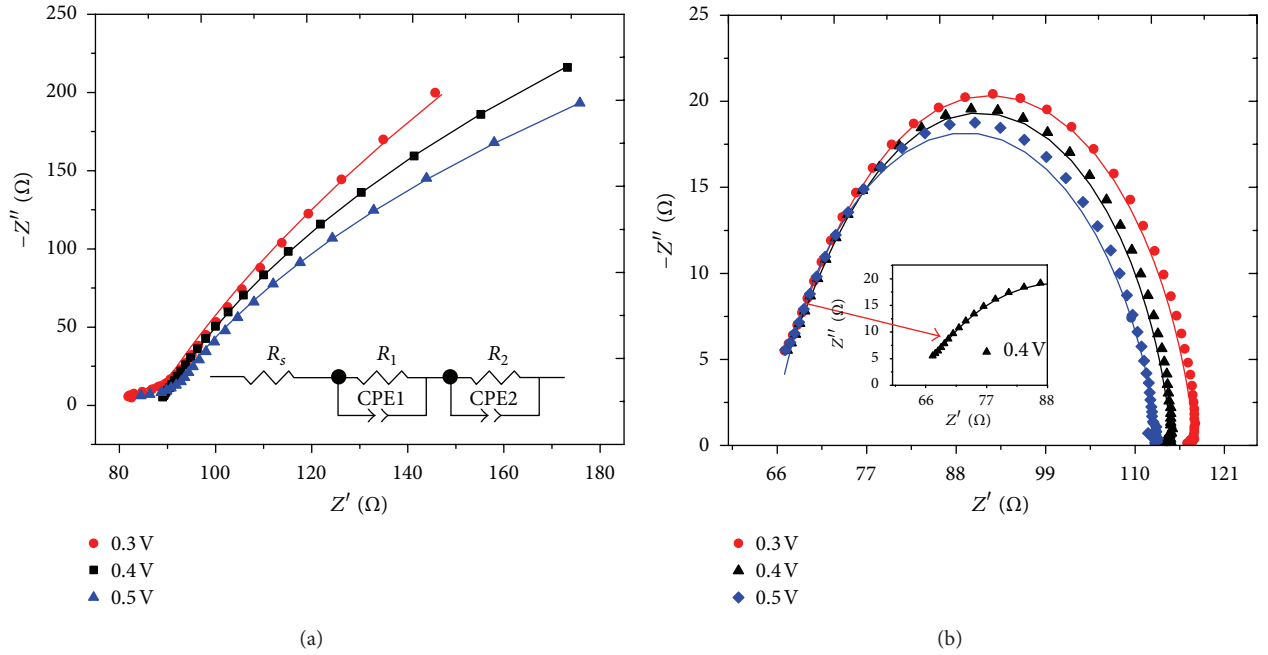

FIGURE 5: Nyquist plots of EIS spectra measured at various applied voltages under illumination of one sun (AM 1.5, 100 mW cm^{-2}) for TiO_2/MPA/CdSe QD (a) and TiO_2/CdSe QD (b) cells. The inset figure in (a) represents the equivalent circuit used for fitting EIS for both cells, while the inset figure in (b) represents the abscissa expanded in the high frequency ranges for TiO_2/CdSe QD cells. The scattered points are experimental data, and the solid lines are the fitting curves.

that the presence of a bifunctional liker (MPA) between the CdSe QDs and TiO_2 layers triggers an interfacial structure with superior ability in inhibiting charge recombination at the electrode/electrolyte interface as a result of the better coverage and higher uniformed CdSe film and the passivation effect of MPA itself, which acts as a blocking effect [3, 34, 43, 44].

The as-prepared QDSSC shows lower conversation efficiency, and one possible reason could be caused by "thick" TiO_2 films, leading the higher interfacial recombination of electrons from TiO_2 and the oxidized form of the redox couples. Another possible reason may be the conduction band alignment of TiO_2 and CdSe quantum dots and injection resistance of excited electron due to MPA. The injection of excited electrons from CdSe quantum dots into TiO_2 is influenced by the energy difference between the two conduction bands. Lower size CdSe QDs have a wider band gap which leads to the absorption of a shorter wavelength of light. However, it is suggested that use of lower size of CdSe QDs can increase the rate of excited electron injection [19]. In the future, we will try to solve the charge transport and injection resistance via preparation of different thickness of TiO_2 films, *in situ* growth of CdSe QDs, and different size of CdSe QDs with different conduction band edge position. Further research using these alternative photoanodes is planned in order to optimize QDSSCs.

4. Conclusion

We demonstrated a new type of photoanode composed of compact and structural layers for QDSSC applications. The compact layer was made of a pure TiO_2 paste, while the structural layer was prepared with PTFE to form a PTFE-framed structure. The overall thickness of the photoanode was measured by SEM: the thickness of the compact layer was ~2 μm, while the structural layer was either 23 or 28 μm. In this photoanode, colloidal CdSe QDs were attached onto the TiO_2 film, both with and without linker molecules (MPA). Different photoanodes with varying total thickness of the TiO_2 film (compact and structural layers) and with varying mode of CdSe QD attachment were prepared. The UV-vis absorption spectra of the as-prepared photoanode show that more CdSe quantum dots were anchored on the MPA surface-modified TiO_2 films suggesting that MPA helped to give a higher coverage of CdSe QDs. From its performance measurement (as shown in I-V curve), energy conversion efficiency up to 0.18% can be achieved for the cell assembled with a TiO_2 (25 μm)/MPA/CdSe QDs photoanode. The electrochemical impedance spectroscopy (EIS) measurements of the highest performance cell were carried out at different applied voltages under one sun illumination. The radius of the semicircle reduced with an increasing applied voltage. The charge recombination resistance of the solar cell prepared with TiO_2 (25 μm)/MPA/CdSe QD photoanode is higher than a cell made with TiO_2 (25 μm)/CdSe QDs photoanode indicating that MPA can help to reduce charge recombination. Furthermore, PTFE in the structural layer formation allows the flexibility to prepare a tunable thickness electrode with a large surface area, and therefore it opens a new opportunity for the simple and cost-effective preparation of TiO_2 electrodes for the large scale preparation of photoanodes.

Conflict of Interests

The authors declare that they have no conflict of interests.

Acknowledgments

The authors gratefully acknowledge the financial support from the National Science Council of Taiwan (NSC-97-2120-M-011-001 and NSC-97-2221-E-011-075-MY3) and the National Taiwan University of Science and Technology (NTUST). The authors are also grateful to the Precious Instrument Center of National Taiwan University of Science and Technology for its support with the TEM measurements.

References

[1] B. O'Regan and M. Grätzel, "A low coast, high-efficiency solar cell based on dye-sensitized colloidal TiO_2 films," *Nature*, vol. 353, pp. 737–739, 1991.

[2] H. Yu, S. Zhang, H. Zhao, B. Xue, P. Liu, and G. Will, "High-performance TiO_2 photoanode with an efficient electron transport network for dye-sensitized solar cells," *Journal of Physical Chemistry C*, vol. 113, no. 36, pp. 16277–16282, 2009.

[3] L.-W. Chong, H.-T. Chien, and Y.-L. Lee, "Assembly of CdSe onto mesoporous TiO_2 films induced by a self-assembled monolayer for quantum dot-sensitized solar cell applications," *Journal of Power Sources*, vol. 195, no. 15, pp. 5109–5113, 2010.

[4] Q. Zhang, Y. Zhang, S. Huang et al., "Application of carbon counterelectrode on CdS quantum dot-sensitized solar cells (QDSSCs)," *Electrochemistry Communications*, vol. 12, no. 2, pp. 327–330, 2010.

[5] J. H. Bang and P. V. Kamat, "Quantum dot sensitized solar cells. A tale of two semiconductor nanocrystals: CdSe and CdTe," *ACS Nano*, vol. 3, no. 6, pp. 1467–1476, 2009.

[6] H. J. Lee, J.-H. Yum, H. C. Leventis et al., "CdSe quantum dot-sensitized solar cells exceeding efficiency 1% at full-sun intensity," *Journal of Physical Chemistry C*, vol. 112, no. 30, pp. 11600–11608, 2008.

[7] Y. Xie, G. Ali, S. H. Yoo, and S. O. Cho, "Sonication-assisted synthesis of CdS quantum-dot-sensitized TiO_2 nanotube arrays with enhanced photoelectrochemical and photocatalytic activity," *ACS Applied Materials and Interfaces*, vol. 2, no. 10, pp. 2910–2914, 2010.

[8] W. Lee, S. K. Min, V. Dhas, S. B. Ogale, and S.-H. Han, "Chemical bath deposition of CdS quantum dots on vertically aligned ZnO nanorods for quantum dots-sensitized solar cells," *Electrochemistry Communications*, vol. 11, no. 1, pp. 103–106, 2009.

[9] B. Farrow and P. V. Kamat, "CdSe quantum dot sensitized solar cells. Shuttling electrons through stacked carbon nanocups," *Journal of the American Chemical Society*, vol. 131, no. 31, pp. 11124–11131, 2009.

[10] Z. A. Peng and X. Peng, "Formation of high-quality CdTe, CdSe, and CdS nanocrystals using CdO as precursor," *Journal of the American Chemical Society*, vol. 123, no. 1, pp. 183–184, 2001.

[11] W. W. Yu, L. Qu, W. Guo, and X. Peng, "Experimental determination of the extinction coefficient of CdTe, CdSe and CdS nanocrystals)," *Chemistry of Materials*, vol. 15, pp. 2854–2860, 2003.

[12] N. S. Lewis, "Toward cost-effective solar energy use," *Science*, vol. 315, no. 5813, pp. 798–801, 2007.

[13] A. J. Nozik, "Multiple exciton generation in semiconductor quantum dots," *Chemical Physics Letters*, vol. 457, no. 1–3, pp. 3–11, 2008.

[14] A. J. Nozik, "Quantum dot solar cells," *Physica E*, vol. 14, no. 1-2, pp. 115–120, 2002.

[15] J.-H. Im, C.-R. Lee, J.-W. Lee, S.-W. Park, and N.-G. Park, "6.5% efficient perovskite quantum-dot-sensitized solar cell," *Nanoscale*, vol. 3, no. 10, pp. 4088–4093, 2011.

[16] T.-L. Li, Y.-L. Lee, and H. Teng, "High-performance quantum dot-sensitized solar cells based on sensitization with $CuInS_2$ quantum dots/CdS heterostructure," *Energy and Environmental Science*, vol. 5, no. 1, pp. 5315–5324, 2012.

[17] V. González-Pedro, C. Sima, G. Marzari et al., "High performance PbS Quantum Dot Sensitized Solar Cells exceeding 4% efficiency: the role of metal precursors in the electron injection and charge separation," *Physical Chemistry Chemical Physics*, 2013.

[18] J. Chen, J. L. Song, X. W. Sun et al., "An oleic acid-capped CdSe quantum-dot sensitized solar cell," *Applied Physics Letters*, vol. 94, no. 15, Article ID 153115, 3 pages, 2009.

[19] A. Kongkanand, K. Tvrdy, K. Takechi, M. Kuno, and P. V. Kamat, "Quantum dot solar cells. Tuning photoresponse through size and shape control of CdSe-TiO_2 architecture," *Journal of the American Chemical Society*, vol. 130, no. 12, pp. 4007–4015, 2008.

[20] Y.-L. Lee and C.-H. Chang, "Efficient polysulfide electrolyte for CdS quantum dot-sensitized solar cells," *Journal of Power Sources*, vol. 185, no. 1, pp. 584–588, 2008.

[21] X. Song, X.-L. Yu, Y. Xie, J. Sun, T. Ling, and X.-W. Du, "Improving charge separation of solar cells by the co-sensitization of CdS quantum dots and dye," *Semiconductor Science and Technology*, vol. 25, no. 9, Article ID 095014, 2010.

[22] C.-H. Chang and Y.-L. Lee, "Chemical bath deposition of CdS quantum dots onto mesoscopic TiO_2 films for application in quantum-dot-sensitized solar cells," *Applied Physics Letters*, vol. 91, no. 5, Article ID 053503, 3 pages, 2007.

[23] S.-C. Lin, Y.-L. Lee, C.-H. Chang, Y.-J. Shen, and Y.-M. Yang, "Quantum-dot-sensitized solar cells: assembly of CdS-quantum-dots coupling techniques of self-assembled monolayer and chemical bath deposition," *Applied Physics Letters*, vol. 90, no. 14, Article ID 143517, 2007.

[24] Y.-L. Lee, B.-M. Huang, and H.-T. Chien, "Highly efficient CdSe-sensitized TiO_2 photoelectrode for quantum-dot-sensitized solar cell applications," *Chemistry of Materials*, vol. 20, no. 22, pp. 6903–6905, 2008.

[25] I. Mora-Seró, S. Giménez, T. Moehl et al., "Factors determining the photovoltaic performance of a CdSe quantum dot sensitized solar cell: the role of the linker molecule and of the counter electrode," *Nanotechnology*, vol. 19, no. 42, Article ID 424007, 2008.

[26] A. Zaban, O. I. Mićić, B. A. Gregg, and A. J. Nozik, "Photosensitization of nanoporous TiO_2 electrodes with InP quantum dots," *Langmuir*, vol. 14, no. 12, pp. 3153–3156, 1998.

[27] P. J. Cameron and L. M. Peter, "Characterization of titanium dioxide blocking layers in dye-sensitized nanocrystalline solar cells," *Journal of Physical Chemistry B*, vol. 107, no. 51, pp. 14394–14400, 2003.

[28] B. Peng, G. Jungmann, C. Jäger, D. Haarer, H.-W. Schmidt, and M. Thelakkat, "Systematic investigation of the role of compact TiO_2 layer in solid state dye-sensitized TiO_2 solar cells," *Coordination Chemistry Reviews*, vol. 248, no. 13-14, pp. 1479–1489, 2004.

[29] H. Yu, S. Zhang, H. Zhao, G. Will, and P. Liu, "An efficient and low-cost TiO_2 compact layer for performance improvement of dye-sensitized solar cells," *Electrochimica Acta*, vol. 54, no. 4, pp. 1319–1324, 2009.

[30] H.-F. Wang, L.-Y. Chen, W.-N. Su, J.-C. Chung, and B.-J. Hwang, "Effect of the compact TiO_2 layer on charge transfer between N3 Dyes and TiO_2 investigated by Raman spectroscopy," *Journal of Physical Chemistry C*, vol. 114, no. 7, pp. 3185–3189, 2010.

[31] H.-F. Wang, W.-N. Su, and B.-J. Hwang, "A novel architecture of poly(tetrafluoroethylene)-framed TiO_2 electrodes for dye-sensitized solar cells," *Electrochemistry Communications*, vol. 11, no. 8, pp. 1647–1649, 2009.

[32] D. W. Ayele, H.-M. Chen, W.-N. Su et al., "Controlled synthesis of CdSe quantum dots by a microwave-enhanced process: a green approach for mass production," *Chemistry A*, vol. 17, no. 20, pp. 5737–5744, 2011.

[33] C. J. Barbé, F. Arendse, P. Comte et al., "Nanocrystalline titanium oxide electrodes for photovoltaic applications," *Journal of the American Ceramic Society*, vol. 80, no. 12, pp. 3157–3171, 1997.

[34] J. Chen, C. Li, D. W. Zhao et al., "A quantum dot sensitized solar cell based on vertically aligned carbon nanotube templated ZnO arrays," *Electrochemistry Communications*, vol. 12, no. 10, pp. 1432–1435, 2010.

[35] R. G. Pearson, "Hard and soft acids and bases," *Journal of the American Chemical Society*, vol. 85, no. 22, pp. 3533–3539, 1963.

[36] K. Mukherjee, T.-H. Teng, R. Jose, and S. Ramakrishna, "Electron transport in electrospun TiO_2 nanofiber dye-sensitized solar cells," *Applied Physics Letters*, vol. 95, no. 1, Article ID 012101, 2009.

[37] I. Bedja, P. V. Kamat, X. Hua, A. G. Lappin, and S. Hotchandani, "Photosensitization of nanocrystalline ZnO films by bis(2,2′-bipyridine)(2,2′-bipyridine-4,4′-dicarboxylic acid)ruthenium(II)," *Langmuir*, vol. 13, no. 8, pp. 2398–2403, 1997.

[38] J. D. Roy-Mayhew, D. J. Bozym, C. Punckt, and I. A. Aksay, "Functionalized graphene as a catalytic counter electrode in dye-sensitized solar cells," *ACS Nano*, vol. 4, no. 10, pp. 6203–6211, 2010.

[39] E. P. A. M. Bakkers, A. L. Roest, A. W. Marsman et al., "Characterization of photoinduced electron tunneling in gold/SAM/Q-CdSe systems by time-resolved photoelectrochemistry," *Journal of Physical Chemistry B*, vol. 104, no. 31, pp. 7266–7272, 2000.

[40] I. Robel, V. Subramanian, M. Kuno, and P. V. Kamat, "Quantum dot solar cells. Harvesting light energy with CdSe nanocrystals molecularly linked to mesoscopic TiO_2 films," *Journal of the American Chemical Society*, vol. 128, no. 7, pp. 2385–2393, 2006.

[41] T. Trupke, P. Würfel, and I. Uhlendorf, "Dependence of the photocurrent conversion efficiency of dye-sensitized solar cells on the incident light intensity," *Journal of Physical Chemistry B*, vol. 104, no. 48, pp. 11484–11488, 2000.

[42] L. Etgar, T. Moehl, S. Gabriel, S. G. Hickey, A. Eychmüller, and M. Grätzel, "Light energy conversion by mesoscopic PbS quantum dots/TiO_2 heterojunction solar cells," *ACS Nano*, vol. 6, no. 4, pp. 3092–3099, 2012.

[43] J. Chen, X. Yang, J. Wu, W. Lei, and X. Zhang, "Enhanced absorption of CdS quantum dots deposited onto ZnO nanorod by using bifunctional linker," *Physica Status Solidi C*, vol. 9, no. 1, pp. 19–21, 2012.

[44] I. Mora-Seró, S. Giménez, F. Fabregat-Santiago et al., "Recombination in quantum dot sensitized solar cells," *Accounts of Chemical Research*, vol. 42, pp. 1848–1857, 2009.